EUROPEAN ORGANIZATION FOR NUCLEAR RESEARCH
CERN - ACCELERATORS AND TECHNOLOGY SECTOR

Magnetic Measurement of the Current Center Line
of the Toroidal Field Coil of ITER at Room Temperature

L. Deniau[1], E. Baynham[2], M. Buzio[1], J. Knaster[3] and F. Savary[1]

1 CERN, Geneva, Switzerland
2 Magnetech Ltd, Didcot, Oxon, United Kingdom
3 ITER, Saint-Paul-Lez-Durance, France

Abstract

Geometrical deformations and assembly errors in the ITER Toroidal Field (TF) coils will lead to magnetic field perturbations, which could degrade plasma confinement and eventually lead to disruption. Extensive computational studies of the influence of coil deformations and assembly errors on plasma behavior have given the basis for definition of the geometric tolerance of the Current Centre Line (CCL) of the winding pack of the TF coil. This paper describes an analysis method to establish the feasibility to measure the magnetic CCL locus of the final winding pack (WP) with accuracy better than 1 mm. The proposed method is based on arrays of gradient coils accurately mounted with respect to the WP fiducial marks and datum surfaces. The magnetic measurements will be performed at defined locations around the WP perimeter to characterize accurately the CCL locus. The analysis emphases the robustness and sensitivity of the method versus the measurement location and the TF coil 3D geometrical deformation. The analysis and proposed measurement techniques will be described in detail.

Magnetic Measurement of the Current Center Line of the Toroidal Field Coil of ITER at Room Temperature

L. Deniau, E. Baynham, M. Buzio, J. Knaster and F. Savary

Abstract— **Geometrical deformations and assembly errors in the ITER Toroidal Field (TF) coils will lead to magnetic field perturbations, which could degrade plasma confinement and eventually lead to disruption. Extensive computational studies of the influence of coil deformations and assembly errors on plasma behavior have given the basis for definition of the geometric tolerance of the Current Centre Line (CCL) of the winding pack of the TF coil. This paper describes an analysis method to establish the feasibility to measure the magnetic CCL locus of the final winding pack (WP) with accuracy better than 1 mm. The proposed method is based on arrays of gradient coils accurately mounted with respect to the WP fiducial marks and datum surfaces. The magnetic measurements will be performed at defined locations around the WP perimeter to characterize accurately the CCL locus. The analysis emphases the robustness and sensitivity of the method versus the measurement location and the TF coil 3D geometrical deformation. The analysis and proposed measurement techniques will be described in detail.**

Index Terms— **ITER, TF coils, field measurement, error fields.**

I. INTRODUCTION

FABRICATION tolerances and assembly misalignments of the ITER Toroidal Field (TF) coils contribute to error fields in the magnetic configuration. These error fields can induce locked modes in the plasma which are operationally critical since they tend to persist once established, eventually bringing the rotating plasma to rest or even causing a disruption [1]. The Three Mode Error Index (TMEI), a weighted parameter of the lowest field harmonics is used as the figure of merit of ITER confinement capability with respect to magnet geometrical deformations and assembly errors. The TMEI has been used for the analysis of the error fields in ITER and the definition of the maximum required currents of the correction coils. The *3-mode* criterion states that $B_{3\text{-mode}}/B_t < 5.0 \ x10^{-5}$, where

$$B_{3\text{-mode}} = \sqrt{0.2B_{1,1}^2 + B_{2,1}^2 + 0.8B_{3,1}^2} \qquad (1)$$

Calculations of plasma behavior have demonstrated that the main contribution will originate from in-plane shifts and tilts of the innermost Central Solenoid coils and radial shifts of the TF coils; the influence of Poloidal Field coils, coil joints,

feeder busbars and presence of ferromagnetic inserts being second order.

The error fields induced by coil tolerances can be accurately calculated through the Current Centre Lines (CCL) of the coils. The CCL of the TF coils can be geometrically defined as the barycenter of the conductor winding geometry in the Winding Pack (WP); its determination is essential to predict the operational conditions of the machine.

The TF coil manufacture will consist of 3 main phases: WP fabrication, insertion of WP in the TF coil cases and closure of the TF coil case with transfer of the CCL reference marking to the external walls [2]. Geometrical tracking of CCL location through these steps is complex. An accurate determination of the coil CCL is important since it becomes the reference for survey operations during the insertion and final installation phase [3]. Therefore, it is considered essential to learn the location of the CCL of the finished WP by undertaking warm magnetic measurements to determine its locus with precision better than 1 mm. This paper describes an analysis method to establish the feasibility of magnetic measurements to this accuracy.

II. TOROIDAL FIELD COIL

The WP, Fig. 1, is the core of the TF magnets with its D-shape weighing 110 tons, measuring about 13 m high and 8 m wide, and with 134 winding turns.
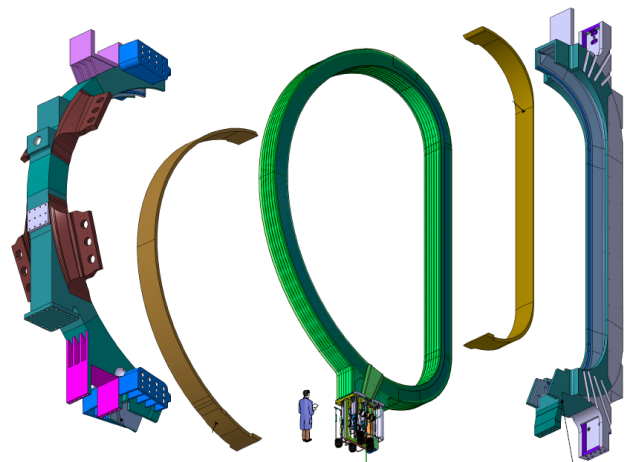

Fig. 1. Insertion of the WP (D-shape) in the cold case of the TF coil.

The nominal current transported by the TF coil conductors made of Nb_3Sn and Cu is 68 kA giving a peak magnetic field of 11.8 T. At room temperature, the TF coil cables can sustain a current of at least 300 A without cooling. The inductance of

the entire TF coil is 0.349 H. The WP is made of seven radial plates, Fig. 2, each supporting one single conductor cable wound in a double pancake.
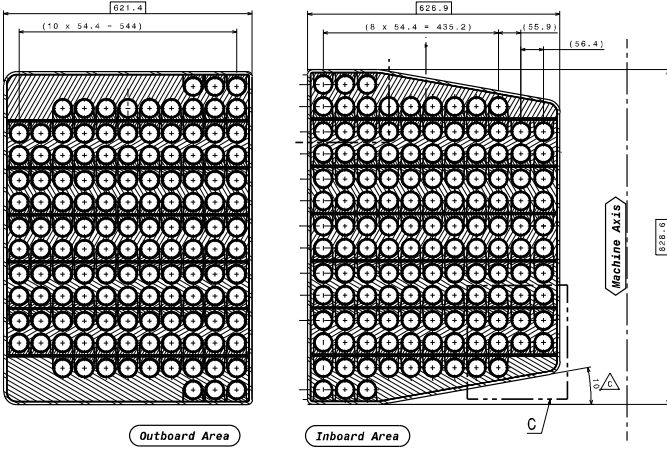

Fig. 2. Cross-section of the inboard (right) and outboard (left) of the 7 radial plates and conductors of the WP.

The CCL is defined as the geometrical barycenter of all the conductors in the cross-section plane (local 2D transverse frame) of the WP [3].

III. DISPLACEMENT ESTIMATE

The measurement principle uses the symmetries of the WP to establish the displacement in the 2D local frame along the TF coil [3]. The Biot Savart law, (2), gives the magnetic flux density generated by a current line,

$$\vec{B} = \frac{\mu_0}{4\pi} \int \frac{I d\vec{l} \times \vec{r}}{|r^3|} \qquad (2)$$

where, I is the current carried by the conductor, dl is the infinitesimal length integrated along the conductor and r is the distance between dl and the point where the magnetic flux density B is considered. The TF field is obtained by summing up the contributions of all conductors expressed in the Cartesian coordinate system of the 2D local frame where the x-axis is pointing inside the TF coil and the y-axis is pointing perpendicularly to the TF coil plane, Fig. 3.

$$B_x(\mathbf{x}) = -\frac{\mu_0}{2\pi} I \sum_i \frac{y - y_i}{r_i^2}$$
$$B_y(\mathbf{x}) = \frac{\mu_0}{2\pi} I \sum_i \frac{x - x_i}{r_i^2} \qquad (3)$$

In order to avoid excessive sensitivity to long-range parasitic magnetic field, all quantities will be based on B_x field measurement, which varies as $1/r^2$ versus x and will limit the contribution of the opposite side of the D-shape.

The δ-displacement can be estimated from the Taylor series expansion of the field B at the reference points $\mathbf{x}$, $\mathbf{x}'$, $\bar{\mathbf{x}}$ and $\bar{\mathbf{x}}'$ around the winding pack, Fig. 3,

$$B(\mathbf{x} + \delta) = B(\mathbf{x}) + J_B(\mathbf{x})\,\delta + \frac{1}{2}\,\delta^T H_B(\mathbf{x})\,\delta + \dots \qquad (4)$$

where J_B and H_B are the field Jacobian and Hessian. Since δ is supposed to be small (~ 1 mm), we can neglect the higher order terms of the series. The field y-symmetries around the
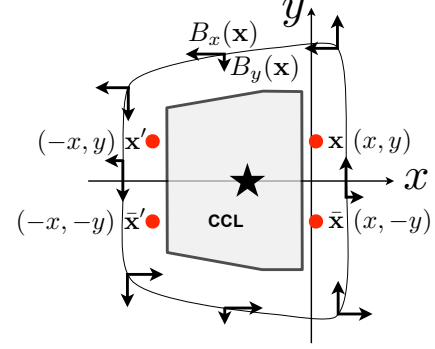
WP, Fig. 3, allow simplifying expressions,

Fig. 3. Symmetries of B and reference points (dots).

$$B_x(\mathbf{x}) = -B_x(\bar{\mathbf{x}}) \quad ; \quad \nabla_x B_x(\mathbf{x}) = -\nabla_x B_x(\bar{\mathbf{x}})$$
$$B_y(\mathbf{x}) = B_y(\bar{\mathbf{x}}) \quad ; \quad \nabla_x B_y(\mathbf{x}) = \nabla_x B_y(\bar{\mathbf{x}}) \qquad (5)$$

while the Cauchy-Riemann equations allow converting B_y gradients into B_x gradients. The δ_y-displacement can be easily expressed in term of B_x and its y-gradient at points $\mathbf{x}$ and $\bar{\mathbf{x}}$, where all measurements include the unknown δ-displacement,

$$\delta_y = \frac{B_x(\mathbf{x} + \delta) + B_x(\bar{\mathbf{x}} + \delta)}{\nabla_y[B_x(\mathbf{x} + \delta) + B_x(\bar{\mathbf{x}} + \delta)]} + O(\delta^2) \qquad (6)$$

The reference points $\mathbf{x}$ and $\bar{\mathbf{x}}$ should be taken far from $y = 0$ (e.g. $y = \pm 0.25$ m) because B_x vanishes there, Fig. 4.
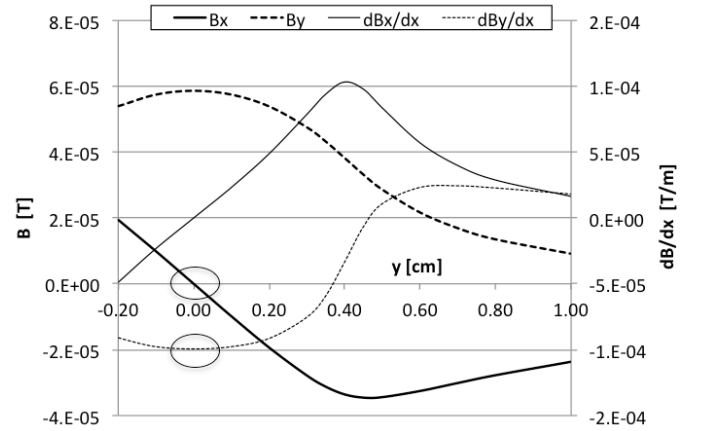

Fig. 4. y-profile of the field and its derivatives at 0.1 m from the inner side of the WP in the inboard area.

The same method can be used for δ_x-displacement, but it requires to approximately recreating the missing x-symmetries of the WP by finding the local x-translation of the pair $(\mathbf{x}, \mathbf{x}')$, such that the following equation holds,

$$\nabla_x B_y(\mathbf{x}) = \nabla_x B_y(\mathbf{x}') \qquad (7)$$

To fulfill this constraint, the measuring system will be moved to the locally predetermined x-position in the WP transverse plane, computed from 3D simulations, before the measurements are performed. Then δ_x-displacement can be approximated by y-gradient and xy-Jacobian of B_x at points $\mathbf{x}$ and $\mathbf{x}'$,

$$\delta_x \approx \frac{\nabla_y[B_x(\mathbf{x} + \delta) - B_x(\mathbf{x}' + \delta)]}{\nabla_{xy}[B_x(\mathbf{x} + \delta) - B_x(\mathbf{x}' + \delta)]} \qquad (8)$$

The motivation for holding *x*-gradient equivalence (7) instead of field equivalence is to avoid problematic long-range B_y terms in the final δ_x-displacement expression.

In both cases, the robustness of the δ-displacement performed at a given pair $(\mathbf{x}, \mathbf{x}')$ can be improved by averaging with its symmetric counterpart $(\bar{\mathbf{x}}, \bar{\mathbf{x}}')$, Fig. 3.

IV. MEASURING SYSTEM

The magnetic flux density can be measured by powering the WP conductors with AC currents and low frequencies (e.g. < 1 Hz) to induce enough voltage in the fixed coil modules centered (Fig. 5, dot) on the reference points (Fig. 3, dots). The coils will be 400 mm long (i.e. TF coil conductor twist pitch) and 15 mm wide with 1000 winding turns giving a magnetic surface of 6 m^2. The relative positional accuracy of the coils inside the modules and the modules inside the measuring system should be known at 10^{-5} m and 10^{-4} m respectively to avoid any significant impact on the estimation of δ within the targeted accuracy of ±1 mm.
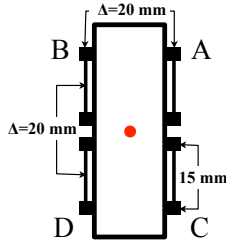

Fig. 5. Schematic module representation with 4 coils.

Finite differences of coils within each module are used to linearly approximate the quantities required to estimate the *x* and *y* components of the δ-displacement,

$$4B_x \approx \mathrm{A} + \mathrm{B} + \mathrm{C} + \mathrm{D}$$
$$2\Delta\nabla_x B_x \approx (\mathrm{A} + \mathrm{C}) - (\mathrm{B} + \mathrm{D})$$
$$2\Delta\nabla_y B_x \approx (\mathrm{A} + \mathrm{B}) - (\mathrm{C} + \mathrm{D})$$
$$\Delta^2\nabla_{xy} B_x \approx (\mathrm{A} - \mathrm{B}) - (\mathrm{C} - \mathrm{D})$$

(9)

where $\Delta = 20$ mm is chosen large enough to ensure enough signal and small enough to ensure good linearity in the region of interest. Faraday's law gives the conversion of varying flux into the induced voltages in the coils,

$$U_x \approx -SN\cos\varphi \times 4\dot{B}_x$$
$$\nabla_y U_x \approx -SN\cos\varphi \times 2\Delta\nabla_y\dot{B}_x$$
$$\nabla_{xy} U_x \approx -SN\cos\varphi \times \Delta^2\nabla_{xy}\dot{B}_x$$

(10)

where SN is the coil magnetic surface, $\dot{B}_x$ is the time varying field and $\cos\varphi = 1$. Then δ-displacement can be expressed in term of the coils induced voltages U_x at the reference points,

$$\delta_x \approx \frac{\Delta\nabla_y[U_x(\mathbf{x}) - U_x(\mathbf{x}') + U_x(\bar{\mathbf{x}}) - U_x(\bar{\mathbf{x}}')]}{2\nabla_{xy}[U_x(\mathbf{x}) - U_x(\mathbf{x}') + U_x(\bar{\mathbf{x}}) - U_x(\bar{\mathbf{x}}')]}$$

$$\delta_y \approx \frac{\Delta[U_x(\mathbf{x}) + U_x(\mathbf{x}') + U_x(\bar{\mathbf{x}}) + U_x(\bar{\mathbf{x}}')]}{2\nabla_y[U_x(\mathbf{x}) + U_x(\mathbf{x}') + U_x(\bar{\mathbf{x}}) + U_x(\bar{\mathbf{x}}')]}$$

(11)

Under room temperature conditions, the measurement acquisition system will have to achieve a precision of ~10^{-6} V per δ_x-mm or δ_y-mm of relative displacement.

V. 3D SIMULATIONS

The validation of the proposed method was performed through the simulation of the measuring system to ensure that 2D approximations are still accurate in 3D [4]. A code has been written for this purpose, using thick polylines with adaptive interpolation to model the TF coil conductors and support field computation for any cable displacements. The geometrical accuracy of the model is guaranteed to be better than 0.1 mm after sampling and displacements. The system simulation has been used on 70 measurement positions along the TF coil to qualify the response of the method to small δ and *step displacement* of the CCL, Fig. 6, left.
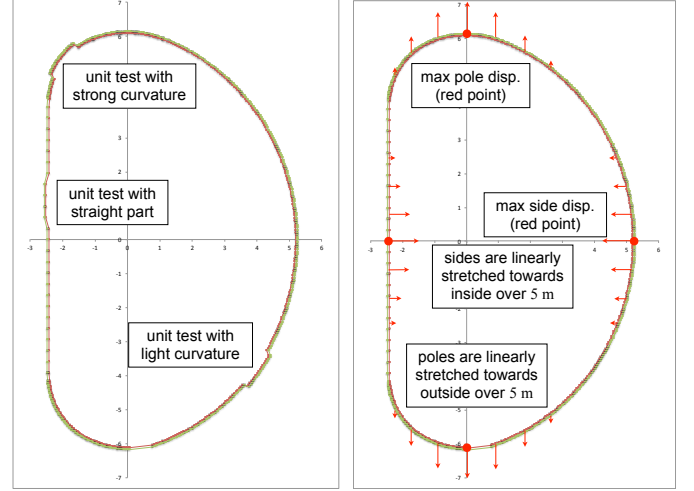

Fig. 6. Step displacements (left) and poles-sides displacements (right) of the TF coil conductors.

The results show that for displacements longer than 3-4 times the length of the measuring coils (i.e. > 1.5 m), the estimation error of the δ-displacement is less than 1% for $\delta = 1\ldots10$ mm. As expected, the estimate of δ_y is more robust than δ_x in transitions area where the sensors partially overlap the displaced regions.
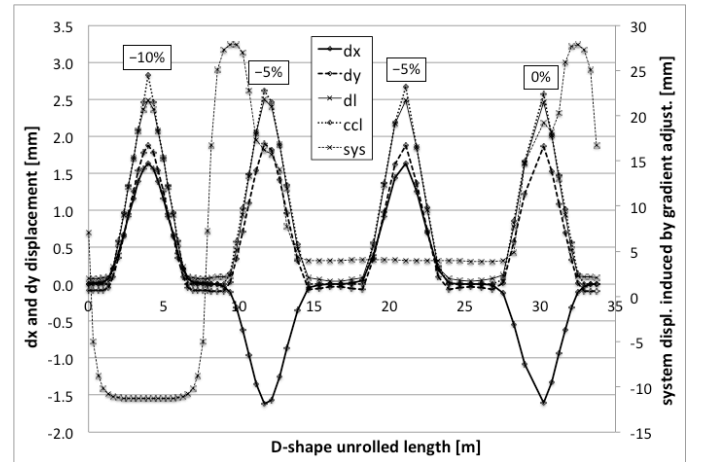

Fig. 7. Simulation of δ-estimates at 70 measurement positions for 2 mm poles and sides displacements.

More realistic cases have been also studied, including TF coil poles and sides stretch, Fig. 6, right, that could occur when the conductors are inserted into the radial plates during

the early assembly phases of the WP.

The simulation results, Fig. 7, show (left scale) the CCL relative displacement and the δ_x, δ_y and δ estimates at each measured position along the TF coil unrolled length and (right scale) the system x-shift adjustment to fulfill gradient equivalence (7). The maximum underestimation of the δ-displacement is about 10% and occurs in the straight part of the TF coil. The 3D simulations have proved that the method is working better than expected despite its simplicity. Moreover, the method was successfully applied to more complex deformations leaving invariant the CCL, proving that the method can be easily adapted to measure other kind of deformations [4].

VI. Sources of Errors

The impact of different error sources on the quality of the measurements, including the effects of eddy currents in the coil itself and the induced magnetization in the surrounding building structures, has been estimated [5].

Poloidal eddy currents are expect to arise in the stainless steel radial plates, where the skin depth is comparable with the dimensions of the cross-section in the frequency range of a few Hz. First, the AC field distribution has been computed via a simplified 2D finite element model, based conservatively on the straight inboard cross-section. The outside field is attenuated by as much as 50% at 2 Hz and still by 10% at 0.5 Hz, which shows that low frequencies (< 1 Hz) are indeed necessary to preserve acceptable signal strength. Due to the asymmetric distribution of the metallic mass, which screens the field more effectively at the inboard, the AC field is not simply attenuated but also distorted leading to an apparent outward displacement of the CCL.

The displacement has been estimated by best-fitting a hyperbolic field profile to the computed $B_y(x,0)$ values in the region $0.5 \text{ m} \leq |x| \leq 2.0 \text{ m}$, which includes the volume where the useful field is generated. In this way we find that, in order to avoid systematic CCL errors above 1 mm, the operating AC frequency must be lower than 0.3 Hz. A reasonable working point can thus be set at 0.2 Hz, which requires a power supply able to provide about 30 A and 20 V. These relatively modest parameters can be provided by a number of inexpensive, commercially available units. The systematic horizontal CCL displacement error, which is about 0.7 mm, can of course be subtracted from the measurement. The result will be affected by the residual uncertainty of the finite element model.

The impact of the steel reinforcement bars embedded in any concrete floor has also been estimated by means of an approximated 2D analytical calculation, taking into account the AC magnetization induced by the TF coil and the resulting field perturbation. The effects of possible eddy current loops occurring within or across the bars, which can in principle be measured and then compensated easily by repeating measurements at different frequencies are not treated here. We have considered a grid of uniformly spaced bars of diameter d, all parallel to the TF coil. This layout is unrealistic but conservative, since transverse bars just channel the magnetic flux away with minimal perturbation above the floor. Each bar, placed at a radial distance r from the coil and immersed in a field H generated by the total current I_{TF}, is magnetized in the direction parallel to H and can be modelled as a dipole of strength per unit length, $N\mu_0 Hd$, where $N = 1/2$ is the demagnetization factor for an infinitely long cylinder. If the TF coil is at height h above the floor, we find that the relative field error at a radial distance ρ from the coil is proportional to $d^2/(h-\rho)^2$, where $d << \rho << h$.

A detailed calculation has been carried out considering a 300 mm thick floor with an overall steel-to-concrete ratio of 8%, housing 20 mm diameter bars with magnetic permeability $\mu_r = 200$, which represents a pessimistic scenario taken from a typical magnet construction hall. The relative field error has been computed for $h = 1.0$ m, 1.5 m and 2.0 m up to one meter distance from the coil, and the consequent CCL position error has been estimated also in this case from an hyperbolic best-fit.

The results indicate that, in all cases considered, the horizontal CCL position is virtually not affected since the error remains smaller than 0.1 mm. On the other hand, the vertical CCL position (depending, in this approximation, upon the horizontal field component only) is more severely affected. By restricting field measurements within a distance of ±0.8 m, however, even in the lowest coil position it is possible to ensure relative field errors smaller than 3%, which translate to CCL position errors smaller than 0.3 mm.

VII. Conclusion

The determination of the Center Current Lines (CCL) of the Toroidal Field (TF) coils is essential to define the coil location in the ITER machine. While geometric definition of the CCL is important and feasible through the Winding Pack (WP) manufacturing steps it is desirable to verify the CCL locus of the final TF WP by magnetic measurement. The principles and accuracy requirements for magnetic measurement of the CCL have been presented. The analysis shows the robustness of the measurement principle for both δ_x and δ_y-displacement modes. The system provides local estimates and is not sensitive to the currents in the other parts of the TF coil.

The proposed measurement system, based on a practical arrangement of four flux coils mounted in a precision module, is able to deliver adequate voltage signal when the TF coil is powered with AC at low frequency. The simulation process developed to check the analysis shows displacement predicttion at the level of ~1% for local displacements and ~10% for global displacements. Sources of errors have been evaluated and shown to be controllable. The feasibility to measure the locus of the CCL of the TF WP with an accuracy of better than 1 mm is demonstrated.

References

[1] J. Knaster, *et al.*, "ITER non-axisymmetric error fields induced by its magnet system", *Fus. Eng. Des.* doi:10.1016/j.fusengdes.2011.02.045
[2] E. Baynham, R. Gallix, J. Knaster, N. Mitchell, and F. Savary, "The Insertion of the WP in the Structural Casing of the TF Coils of ITER", *IEEE Trans. on Applied Supercond.,* 20 (3) 2010.
[3] J. Knaster and E. Baynham, The Determination of the Current Center Line of the TF Coils of ITER, *IEEE Trans. on Applied Supercond.* 20 (3), 2010.
[4] L. Deniau, "Magnetic Measurements of the Center Current Line at Room Temperature", *CERN-ITER Technical Report, unpublished*, 2011.
[5] M. Buzio, Addendum to [4], *CERN-ITER Technical Report*, 2011.